Vol. 81, No. 3, 1978 BIOCHEMICAL AND BIOPHYSICAL RESEARCH COMMUNICATIONS
April 14, 1978 Pages 955-964

STOPPED FLOW KINETICS OF CARBAMYLCHOLINE BINDING TO MEMBRANE BOUND ACETYLCHOLINE RECEPTOR

U. Quast, M. Schimerlik and M.A. Raftery

Church Laboratory of Chemical Biology
Division of Chemistry and Chemical Engineering
California Institute of Technology
Pasadena, California 91125

Received November 11, 1977

SUMMARY: Conformational changes upon binding of carbamylcholine to acetylcholine receptor-enriched membrane fragments have been observed by stopped-flow methods using the fluorescent probe ethidium bromide. A model consistent with both equilibrium and kinetic experiments is proposed in which the receptor binds two molecules of carbamylcholine with high affinity in a non-cooperative manner followed by binding of a third and possibly a fourth molecule with increasingly lower affinity. The receptor ligand precomplexes isomerize to different non-interconvertible complexes depending on the number of ligands bound. This kinetic model fits the data for carbamylcholine interactions with receptor prepared initially either in a low or high affinity form for ligands.

INTRODUCTION

Mechanistic studies of conformational changes in acetylcholine receptor-rich membrane fragments upon ligand binding have been conducted using intrinsic fluorescence (1,2), extrinsic fluorescent probes (3,4) and by time-dependent changes in affinity for cholinergic ligands detected by inhibition of [^{125}I]-α-bungarotoxin binding kinetics (5-8). In the present study a comparison is made of Torpedo californica acetylcholine receptor-rich membranes that were initially in low affinity and high affinity forms for carbamylcholine; the low affinity membranes decayed to the high affinity form within a few days. We describe quantitatively conformational changes observed by virtue of an increase in ethidium fluorescence after carbamylcholine bound to the receptor-ethidium complex, in either the high or low affinity forms. The

Supported by USPHS Grant NS-10294, by a Fellowship from the Deutsche Forschungsgemeinschaft (to U.Q.), and an NIH Postdoctoral Fellowship (to M.S.)
Contribution #5644

0006-291X/78/0813-0955$01.00/0

proposed model describes the relationship between the observed kinetics and the number of carbamylcholine molecules bound to the membrane bound acetylcholine receptor.

MATERIALS AND METHODS

Torpedo californica acetylcholine receptor-enriched membrane fragments were prepared as described previously (9,10) and the concentration of α-bungarotoxin sites determined by the method of Schmidt and Raftery (11). The affinity of membrane-bound acetylcholine receptor for carbamylcholine was characterized by the inhibition by carbamylcholine of the initial rate of [^{125}I]-α-toxin receptor complex formation with and without preincubation (for assay details see 7,8).

Rapid kinetic experiments were done on a Durrum stopped-flow photometer equipped with a soft stop. Exciting light was at 493 ± 4 nm and emission was monitored using a Corning C.S. 3-69 cut-off filter. Membrane fragments, 0.5 μM in toxin sites, plus 2 μM ethidium bromide were mixed with 2 μM ethidium bromide plus carbamylcholine in order to maintain a constant indicator concentration. The traces were recorded with a Hewlett Packard 7004-B x-y recorder or a Tektronix 5103N oscilloscope and were analyzed by hand. Equilibrium binding studies with [^{3}H]-carbamylcholine and [^{3}H]-ethidium were conducted by centrifugation assay.

Ethidium bromide was purchased from Cal Biochem and carbamylcholine chloride from Sigma-Chemical Co. The syntheses of [^{3}H]-carbamylcholine and [^{3}H]-ethidium bromide (specific activities 57 mCi/mmole and 100 mCi/mmole respectively) will be described elsewhere. All experiments were performed in Torpedo Ringers containing 0.02% w/v sodium azide at pH 7.4 and 25°C.

RESULTS

Equilibrium Measurements of [^{3}H]-Carbamylcholine Binding:

Scatchard plot data for the binding of [^{3}H]-carbamylcholine to low affinity acetylcholine receptor (5-8) in the presence and absence of 2 μM ethidium (Figure 1) show that at equilibrium there are one half as many high affinity carbamylcholine sites as α-bungarotoxin sites. Assuming that there are four toxin sites per membrane receptor (17), this indicates that two molecules of carbamylcholine bind with high affinity. The linear slopes (Figure 1) indicate one homogeneous class of noninteracting binding sites for carbamylcholine with equilibrium constants K_D = 65 nM (Figure 1A) or 80 nM (Figure 1B) respectively. Similar data were obtained with receptor originally in the high affinity form. The data are compatible with a third molecule of ligand binding with substantially lower affinity as required by the kinetic experiments (see below). Comparison of Figure 1A and 1B shows that 2 μM ethidium had only a small effect on the affinity of carbamylcholine binding and no effect on the number of binding sites.

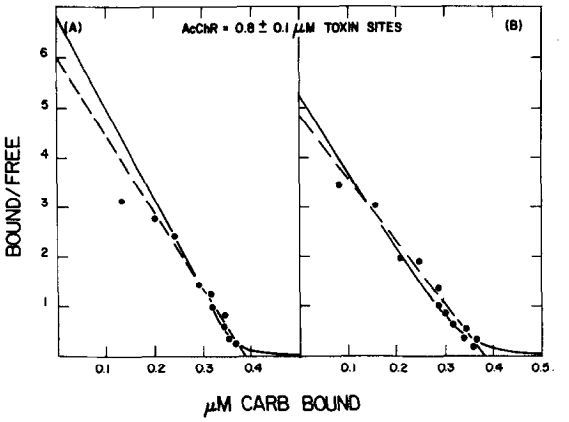

FIGURE 1: Scatchard Plot of [^{3}H]-Carbamylcholine Binding to Acetylcholine Receptor: Ethidium bromide concentrations in (A)=0, (B)=2 μM. Experiments were done by centrifugation assay. [Receptor] was 0.8 ± 0.1 μM in toxin sites. --- Linear least squares analysis of the data. From the abscissa intercepts the ratio of ligand to toxin sites equals 0.49 for (A) and (B). K_d = 65 nM (A) or K_d = 80 nM (B). —— Curve calculated according to scheme (1) neglecting binding of the fourth ligand. Parameters used: [receptor] = 0.7 μM in toxin sites, (A) K_1K_1' = 0.05 μM, $K_1K_2K_3K_3$ = 2.8×10^{-2} μM^3 and (B) K_1K_1' = 0.07 μM, $K_1K_2K_3K_3'$ = 2.8×10^{-2} μM^3.

Ethidium as an Indicator:

We have previously shown (4) that the observed increase in ethidium fluorescence intensity upon the binding of carbamylcholine arises specifically from the receptor-ethidium-carbamylcholine complex. The addition of carbamylcholine to [^{3}H]-ethidium receptor complex does not lead to an increase in concentration of dye bound indicating that the observed increase in fluorescence is due to a change in quantum yield of ethidium bromide bound in the ternary complex rather than to dye uptake (manuscript in preparation).

Kinetic Titration of Membrane Fragments in the High Affinity Form with Carbamylcholine:

Rapid mixing of membrane fragments plus 2 μM ethidium with 2 μM ethidium in the stopped-flow photometer resulted in an essentially flat baseline

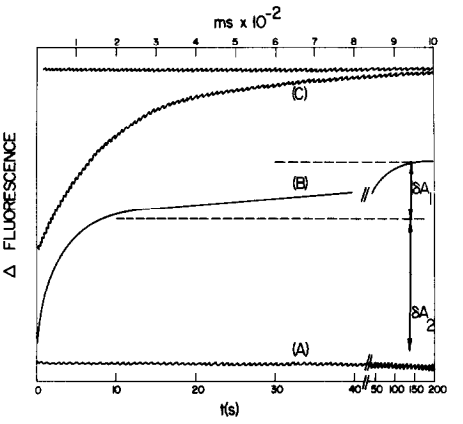

FIGURE 2: **Kinetic Traces of Fluorescence Intensity Increase of Ethidium Bromide Upon Rapid Mixing of Receptor with Carbamylcholine in a Stopped-Flow Photometer:** One syringe contained receptor (0.5 μM in toxin sites, originally in the high affinity form) and 2 μM ethidium bromide and the amount of carbamylcholine indicated below. (A) Control: [Carbamylcholine] = 0. The same flat baseline was observed when acetylcholine receptor-α-bungarotoxin complex was mixed with carbamylcholine. (B) [Carbamylcholine] = 3 μM. The faster phase (δA_2) is followed by the slower phase δA_1. Evaluation of the data gave $\delta A_1/\delta A_t = 0.3$, $\tau_1^{-1} = 1.8 \times 10^{-2}$ s^{-1}, $\delta A_2/\delta A_t = 0.7$, $\tau_2^{-1} = 0.42$ s^{-1}. (C) [Carbamylcholine] = 2 mM, time scale 100 ms/div. The semilog plot of the data revealed two phases (2 and 3) with $\delta A_2/\delta A_t = 0.46$, $\tau_2^{-1} = 3.5$ s^{-1} and $\delta A_3/\delta A_t = 0.54$, $\tau_3^{-1} = 18$ s^{-1}.

(Figure 2). When membrane fragments were mixed with carbamylcholine concentrations lower than 1 μM the observed increase in ethidium fluorescence followed a single exponential with an apparent half-time in the minute range (Phase 1). Above 1 μM carbamylcholine, a faster phase (Phase 2) arose (Figure 2). Figure 4 shows that Phase 2 increased in both rate and amplitude with increasing ligand concentration. Correspondingly, both the apparent rate constant τ_1^{-1} (Figure 3, -O-) and relative amplitude δA_1 (Figure 3,-▲-) of Phase 1 decreased. At very high carbamylcholine concentrations a much faster phase (Phase 3) appeared at the expense of Phase 2 (see Figures 2,4).

The observation of a single exponential at ligand concentrations less than 1 μM where the equilibrium binding data (Figure 1) indicate the existence of mono-and diliganded receptor complexes C_1 and C_2 implies that the

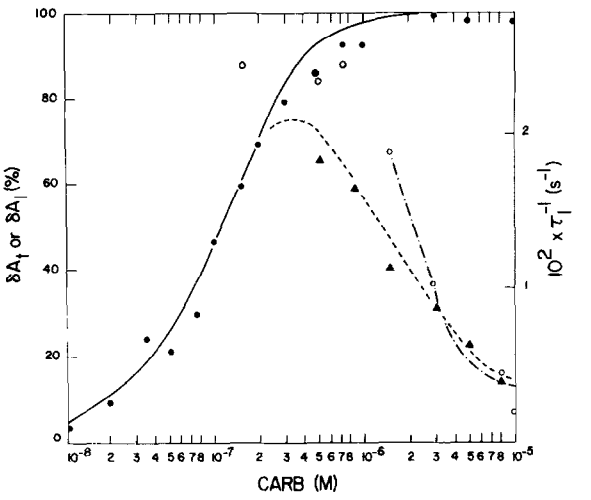

FIGURE 3: **Dependence of Total Amplitude and Phase 1 on Total Carbamylcholine Concentration: (-●-) δA_t, (-▲-) δA_1 and (-O-) τ_1^{-1}. Conditions were as indicated in Figure 2. Curves shown as ——, ---, -•-, were calculated according to Equations (A6), (A2a) and (A4) respectively using the parameters given in Table 1.**

formation of both these complexes is observed in the single slow kinetic phase (Phase 1). The concentration dependence of the kinetic parameters of Phases 1 and 2 (see Figures 3,4) can be quantitatively accounted for by assuming formation of a tri-liganded complex C_3 at ligand concentrations above 1 μM, as reflected in Phase 2 (Figure 4). With increasing ligand concentration, formation of C_3 is favored by the law of mass action at the expense of $C_1 + C_2$, thus leading to a decrease in both amplitude δA_1 and apparent rate constant τ_1^{-1} of Phase 1 (see Figure 3). At concentrations well below 1 μM, where formation of C_3 can be neglected, δA_1 increased with increasing ligand concentration, reflecting increasing saturation of $C_1 + C_2$ whereas the apparent rate constant τ_1^{-1} was almost independent of the ligand concentration since ligand was not in excess over receptor (see Figure 3). The amplitude δA_2 and the rate constant τ_2^{-1} of the second phase (which reflects the formation of C_3) both increased with increasing ligand concentration until reaching a plateau (see Figure 4). The total amplitude $\delta A_t = \delta A_1 + \delta A_2$ (see Figure 3, -●-) followed a binding hyperbola and remained constant at

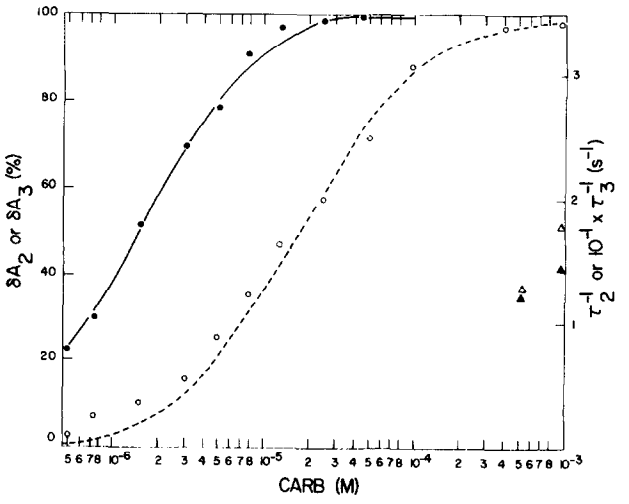

FIGURE 4: **Dependence of Phase 2 and 3 on Total Carbamylcholine Concentration:** δA_2 (-●-), τ_2^{-1} (-○-), δA_3 (-▲-) and τ_3^{-1} (-△-). Conditions as in Figure 2. —— and --- are curves calculated according to Equations (A3a) and (A5).

ligand concentrations greater than 2 μM, indicating that formation of $C_1 + C_2$ was accompanied by the same fluorescence enhancement as formation of C_3. At ligand concentrations approaching 1 mM (Figure 2, top trace and Figure 4) the fastest kinetic phase appeared (Phase 3) at the expense of Phase 2. We tentatively attribute this to the formation of the tetra-liganded receptor (C_4) although we do not have enough data to treat this point quantitatively. Omitting bound ethidium the proposed mechanism can be written:

$$R + 4L \underset{}{\overset{K_1}{\rightleftharpoons}} RL + 3L \overset{K_2}{\rightleftharpoons} RL_2 + 2L \overset{K_3}{\rightleftharpoons} RL_3 + L \overset{K_4}{\rightleftharpoons} RL_4$$

$$RL \;(k_1' \uparrow\downarrow k_{-1}') \; C_1 \qquad RL_2 \;(k_2' \uparrow\downarrow k_{-2}') \; C_2 \qquad RL_3 \;(k_3' \uparrow\downarrow k_{-3}') \; C_3 \qquad RL_4 \;(k_4' \uparrow\downarrow k_{-4}') \; C_4$$

SLOW FASTER (FASTEST)

where R = receptor, L = carbamylcholine, RL_i the receptor-ligand precomplex and C_i the final receptor ligand complex with i molecules of ligand bound (i=1,...,4). Depending on ligand concentration, the receptor first combines in a fast step with i ligand molecules to form RL_i followed by a slow isomerization to the final complex C_i. On the time scale of the experiment C_i

TABLE 1

PARAMETERS DERIVED FROM FITTING THE DATA IN FIGURES 3 AND 4 TO SCHEME (1) ACCORDING TO THE FORMULAE LISTED IN THE APPENDIX

(Values in parentheses refer to experiments with receptor originally in the low affinity form with $[receptor]_o$ = 0.15 μM in toxin sites)

K_1K_1' = 0.1 μM (0.2 μM); K_1 = 2 μM (≃ 2.5 μM); k_1' = 0.95 s^{-1} (0.2 s^{-1}).
K_2 = 0.75 μM (≃ 3.6 μM)
$K_1K_2K_3K_3'$ = 0.013 μM^3 (0.1 μM^3); K_3 = 14 μM (≃ 100 μM); k_3' = 3.5 s^{-1} (> 2.5 s^{-1})
Quantum yields Q_i = Q
saturation amplitude δA_t = 7.6% at $[receptor]_o$ = 0.25 μM toxin sites (4.2% at $[receptor]_o$ = 0.15 μM) with a total fluorescence corresponding to 9.6 V.

does not bind further ligands. The increase in fluorescence arises in the isomerization steps $RL_i \rightarrow C_i$ and the fluorescence enhancement is the same for all C_i. A complete analysis of scheme (1) in terms of two exponentials will be given elsewhere. The formulae necessary for a fit of the experimental data in Figures 3 and 4 to mechanism 1 are listed in the Appendix and the fitting parameters are given in Table 1. These parameters varied up to a factor of 2 for different preparations. The data do not allow for a fourth ligand to bind at carbamylcholine concentrations less than 50 μM.

The kinetic behavior of carbamylcholine binding to the receptor originally in the low affinity form was similar to that obtained with high affinity membranes. The fit of these data to mechanism 1 gave the parameter values (in parentheses) in Table 1.

DISCUSSION

The absence of any fluorescence enhancements in the presence of a saturating concentration of α-toxin (see Caption of Figure 2) strongly indi-

cates that the observed signal arose from interactions between carbamylcholine and the receptor ethidium complex. Since the kinetics were both too slow and saturable by the ligand, neither kinetic phase reflects the direct ligand binding step. The signal was assumed to arise from slow isomerizations of the ternary complexes after ligand binding, causing a change in micro-environment of the bound ethidium. Any mechanism which describes the kinetic data must accommodate a linear Scatchard plot extrapolating towards one half of the toxin sites with the observed complex kinetic behavior developing at concentrations where binding of the first two ligands was almost complete. The possibility that the same diliganded complex was formed via different kinetic pathways depending on ligand concentration is inconsistent with the concentration dependence of the amplitudes. Simple sequential (12) and two state models (13) can also be excluded. The kinetic data seem compatible only with the parallel formation of complexes with different states of ligation (scheme 1). A formally similar scheme with only two ligand molecules binding has been proposed for the acetylcholine receptor at the frog neuromuscular junction (14).

The value of the overall dissociation constant for the first two ligands $K_1K_1' = 100$ nM is in good agreement with the equilibrium data in Figure 1 and with published values (8,17). The value of the preequilibrium constant $K_1 = 2.0$ μM is, however, one order of magnitude smaller than other reported values (2,8,16).

The kinetic scheme predicts binding of a third ligand with an apparent equilibrium constant of 1.5 μM. The equilibrium data in Figure 1 are compatible with this requirement. More direct evidence for a third (and fourth) ligand binding is desirable although technically difficult to obtain due to non-specific binding of the ligand to the membrane.

The most important result of this study is that the kinetics of the interaction of membrane bound acetylcholine receptor with carbamylcholine as reflected by ethidium fluorescence can be fitted to the same kinetic scheme

(1). This makes it difficult to relate the observed phenomena to in vitro desensitization (1-3, 5-8) or "channel opening" (3). It clearly shows, however, that carbamylcholine induced conformational changes both in high and low affinity acetylcholine receptor in vitro.

APPENDIX

Scheme (1) was analyzed neglecting binding of the fourth ligand. Linearity of the Scatchard plot data requires $(K_1K_1')^2 = K_1K_2K_2'$. Assuming that the quantum yields Q_i are identical for all C_i, $Q_i = Q$, and that $k'_{-1} = k'_{-2}$, the increase in fluorescence is given by ($\tau_1^{-1} << \tau_2^{-1}$):

$$z = Q[(\bar{C}_1+\bar{C}_2+\bar{C}_3) + \delta A_1 \exp(-t/\tau_1) + \delta A_2 \exp(-t/\tau_2)] \quad (A1)$$

with

$$\delta A_1 = Q[(\bar{C}_1+\bar{C}_2)(-1+(\tau_1 k'_{-2})^{-1}) + \bar{C}_3(-1+(\tau_1 k'_{-1})^{-1})] \quad (A2)$$

$$\delta A_2 = -Q[(\bar{C}_1+\bar{C}_2)(\tau_1 k'_{-2})^{-1} + \bar{C}_3(\tau_1 k'_{-1})^{-1}] \quad (A3)$$

$$(\bar{C}_1+\bar{C}_2) = R_o[2L/(K_1K_1') + L^2/(K_1K_1')^2]\alpha^{-1},\ \bar{C}_3 = R_o[L^3/(K_1K_2K_3K_3')]\alpha^{-1}$$

where $\alpha = (1+L/K_1K_1')^2 + L^3/(K_1K_2K_3K_3')$ and the bars denote concentrations at equilibrium. The respective relaxation times are given by:

$$\tau_1^{-1} = k'_{-1} + [k_1'(2L/K_1+L^2/(K_1^2K_1'))]\ [1+2L/K_1+L^2/(K_1K_2)+L^3/(K_1K_2K_3K_3')]^{-1} \quad (A4)$$

$$\tau_2^{-1} = k'_{-3} + [k_3'L^3/(K_1K_2K_3)]\ [1+2L/K_1+L^2/(K_1K_2)+L^3(K_1K_2K_3)]^{-1} \quad (A5)$$

and

$$\delta A_t \equiv \delta A_1 + \delta A_2 \quad (A6)$$

For this preliminary evaluation of the data the amplitudes were approximated by:

$$\delta A_1 \simeq -Q(\bar{C}_1+\bar{C}_2) \quad (A2a)$$

$$\delta A_2 \simeq -Q\,\bar{C}_3 \quad (A3a)$$

A more rigorous treatment of the data is now in progress.

ACKNOWLEDGMENTS

The authors would like to express their thanks to Professor T. Jovin for helpful discussions and to Mr. J. Racs for his technical assistance.

REFERENCES

1. Barrantes, F.J. (1976) Biochem. Biophys. Res. Comm. 72, 479-488.
2. Bonner, R., Barrantes, F.J. and Jovin, T.M. (1976) Nature 263, 429-431.

3. Grünhagen, H.H. and Changeux, J.-P. (1976) J. Mol. Biol. 106, 479-516 and 517-535.
4. Schimerlik, M.I. and Raftery, M.A. (1976) Biochem. Biophys. Res. Comm. 73, 607-613.
5. Weber, M., David-Pfeuty, Th. and Changeux, J.-P. (1975) Proc. Natl. Acad. Sci. USA 72, 3443-3447.
6. Weiland, G., Georgia, B., Wee, V.T., Chignell, C.F. and Taylor, P. (1976) Mol. Pharmacol. 12, 1091-1105.
7. Lee, T., Witzemann, V., Schimerlik, M.I. and Raftery, M.A. (1977) Arch. Biochem. Biophys. 183, 57-63.
8. Quast, U., Schimerlik, M.I., Lee, T., Witzemann, V., Blanchard, S. and Raftery, M.A. (1977) Biochemistry, in press.
9. Duguid, J.R. and Raftery, M.A. (1973) Biochemistry 12, 3693.
10. Reed, K., Vandlen, R., Bode, J., Duguid, J. and Raftery, M.A. (1975) Arch. Biochem. Biophys. 167, 138-144.
11. Schmidt, J. and Raftery, M.A. (1973) Anal. Biochem. 52, 349-354.
12. Loudon, G.M. and Koshland, D.E. (1972) Biochemistry 11, 229-240.
13. Janin, J. (1973) Progr. Biophys. 27, 77-120.
14. Stevens, C.F., (1975) in Cold Spring Harbor Symp. Quant. Biol., XL (The Synapse), Cold Spring Harbor, New York, p. 169-173.
15. Weber, M. and Changuex, J.-P. (1974) Mol. Pharmacol. 10, 15-34.
16. Moreau, M. and Changeux, J.-P. (1976) J. Mol. Biol. 106, 457-467.
17. Raftery, M.A., Vandlen, R.L., Reed, K.L. and Lee, T. (1975) , Cold Spring Harbor Symp. Quant. Biol., XL (The Synapse, Cold Spring Harbor, New York, p. 193-202.